

Morphological Studies in Thermally Initiated Emulsion (Co)polymerization without Conventional Initiators

YONG-ZHONG DU, GUANG-HUI MA, HEN-MEI NI, MASATOSHI NAGAI, SHINZO OMI

Graduate School of Bio-Applications and Systems Engineering, Tokyo University of Agriculture and Technology, Koganei, Tokyo 184-8588, Japan

Received 28 May 2001; accepted 28 August 2001

ABSTRACT: Poly(methyl methacrylate-co-styrene) composite latices were prepared by thermally initiated seed emulsion (co)polymerization of styrene (ST), methyl methacrylate (MMA), or ST and MMA employing a PST or PMMA seed in the absence of conventional initiators. The changes of particle morphology, observed by transmission electron microscopy (TEM), were investigated by varying seed particle component, the weight ratio of monomer to seed polymer, monomer composition, and employing pre-swelling of the seed particles. The size distribution of polymer particles obtained from thermally initiated emulsion (co)polymerization was improved by employing the seed process. Hemisphere-like, sandwich-like, core-shell, and inverted core-shell particle morphologies were observed depending upon the polymerization conditions. The pre-swelling of seed particles did not affect the morphology of final particles. The particle morphologies, obtained from the thermal process, were compared with those obtained from conventional seed emulsion polymerization. The incorporation of an initiator fragment SO_4^- to polymer chain ends seemed to allow the PST chains to gain some hydrophilicity. From the observation of particle morphology, the hydrophilicity of involved polymers were in the following order: PMMA with ionic ($-\text{SO}_4^-$) chain ends > PMMA with no ionic ends > PST with ionic ends > 60% MMA P(MMA-co-ST) with no polar ends > 40% MMA P(MMA-co-ST) with no polar ends > PST with no polar ends. © 2002 Wiley Periodicals, Inc. *J Appl Polym Sci* 84: 1737–1748, 2002; DOI 10.1002/app.10581

Key words: morphology; thermal initiation; emulsion polymerization; styrene; methyl methacrylate

INTRODUCTION

There has been much industrial interest in controlling latex particle morphology. Usually, the formation of unique multicomponent heterogeneous structures can be obtained by the seed emulsion polymerization technique. Formulations for multicomponent, heterogeneous particle structures, with characteristics unlike those of the random copolymer or polymer blend, create a more versatile class of materials. Composite latices

are utilized in end-use applications such as architectural and automotive coatings, impact modifiers in advanced engineering plastics to improve the impact strength and toughness, adhesives to provide optimum peel strength, and many other sophisticated products for areas such as membrane separation and biotechnology.

Reflecting the kinetics of emulsion polymerization proposed by Smith and Ewart,¹ their Case 2 predicts that the average number of free radicals per particle is 0.5, and consequently, the rate of polymerization stays constant provided that the number of polymer particles is constant and the equilibrium swelling of monomer is guaranteed during the presence of monomer droplets. The

Correspondence to: S. Omi (omi@cc.tuat.ac.jp).

Journal of Applied Polymer Science, Vol. 84, 1737–1748 (2002)
© 2002 Wiley Periodicals, Inc.

theory presumes a uniform size of polymer particles and that colloidal stability is well maintained. The evidence that the average number of free radicals per particle is equal to 0.5 for monomer conversions up to 60% was provided by initiator perturbation studies. The initiator concentration of a run in progress was suddenly doubled, and the observed invariance in the polymerization rate confirmed that the average number of free radicals per particle is equal to 0.5 and remains constant. Due to this argument, Williams et al.²⁻⁴ proposed the hypothesis that the polymerization occurs in a monomer-rich shell of relatively constant monomer concentration. They proposed the nonuniform "core-shell" theory of particle growth in the seed emulsion polymerization of styrene onto polystyrene seed particles, and postulated that a "core-shell" structure, similar to those morphologies that were developed in systems in which the seed polymer and the secondary polymer were inherently incompatible, was also formed in the emulsion polymerization of a compatible monomer-polymer system.

However, Williams's "core-shell" theory of particle growth led to many unresolved arguments. Napper⁵ pointed out that the diffusion rates of the species present within the polymer particle did not support the hypothesis for such large differences in the monomer concentrations between the core and shell, but he generally agreed with the morphological evidence presented by Williams, and proposed an alternate hypothesis that later was experimentally supported by Vanderhoff's data.⁶ In this hypothesis, the surface-active oligomeric radicals formed in the aqueous phase by the decomposition of the water-soluble initiator and the addition of monomer molecules, adsorb onto the particle surface and become incorporated in the particles by continuing to add new monomer molecules. The monomer molecules can diffuse readily through a viscous medium, while the large polymer radicals diffuse only slowly under the same conditions. Therefore, the newly formed polymer chains are likely to remain closer to the particle surface, even though the monomer is distributed homogeneously throughout the particle.

Moreover, Chern and Poehlein^{7,8} considered that the nonuniform core-shell type of morphology resulted from a nonuniform distribution of free radicals in the particles. The polar end groups of growing polymer chains attached on the particle surface, and the radical concentration were statistically higher near the particle surface. Gilbert et al.⁹ pointed out that a radical pair

generated near the particle surface could easily be separated by the desorption of one radical into the aqueous phase, which would locally increase the initiation efficiency. Moreover, at the surface, the single radicals entering the particles from the aqueous phase would increase the local radical concentration.

Shen et al.¹⁰ demonstrated the existence of a shell polymerization process, even in the case where a nonpolar initiator like 2,2'-azo(bisisobutyronitrile) (AIBN) was used, which would not restrict the polymer chain ends to remain attached at the particle-water interface. They indicated that the surface and internal domains were generated under different conditions. Surface domains were always produced under conditions where the particles exhibited a high viscosity, primarily during the later stages of polymerization. In poly(methyl methacrylate)-seed emulsion polymerization of styrene, Cho and Lee¹¹ showed that the anchoring effect exerted by ionic terminal groups introduced by ionic initiator was found to be the main factor in controlling the particle morphology. An oil-soluble hydrophobic initiator and water-soluble but less hydrophilic initiator gave inverted core-shell morphology. When water-soluble hydrophilic initiator was employed, the particle morphology changed from hemispherical, sandwich-like to core-shell type.

Thermally initiated emulsion polymerization without conventional initiators has been investigated by many researchers,¹²⁻¹⁵ but its mechanism was largely neglected. The application of such latices has not been extensively publicized. We have been investigating the kinetics of this system for some years.¹⁶⁻¹⁸ Because no initiators were used, the polymerization rate was very low, and led to polydispersity of the polymer particles. The polydispersity of the polymer particles is an advantage for producing high solids polymer latices.^{19,20} Recently, high solid content latices, as high as 70%, have been prepared by thermally initiated emulsion polymerization of styrene.²¹

Because no initiators are used, the polymer chain ends do not contain any initiator fragments; therefore, it is expected to yield different morphological form, compared with the conventional initiator system. On the other hand, if the morphology obtained from the thermally initiated seed emulsion polymerization can be controlled, the application of such latices will be extended, and provide some aid to clarify the thermally initiated emulsion polymerization mechanism as well. In this article, the particle morphologies ob-

Table I Recipes for Preparation of Seed Polymer Particles

Run No.	ST (g)	MMA (g)	SDS (g)	APS (g)	Water (g) ^a
1901	/	300	3.0	0.3	700
1902	300	/	3.0	0.3	700

The reaction temperature is 343 K, and the reaction time is 4 h.

^aThis amount is including SDS (g) and APS (g).

tained by thermally initiated seed emulsion polymerization were investigated by comparing with the particle morphologies obtained from conventional seed emulsion polymerization. As shown later, an advantage of the thermally initiated seed emulsion polymerization is that it can provide polymer chains with the ends free of initiator fragments in the seed particles prepared by using conventional initiators.

EXPERIMENTAL

Material

All the reagents, unless stated otherwise, were purchased from Kishida Chemical. Co. Methyl methacrylate (MMA) and styrene (ST) monomers were commercial grade, and distilled under reduced pressure. In all runs, fresh MMA and ST were used immediately after distillation. Sodium dodecyl sulfate (SDS, biochemistry grade, Merck Co.), and ammonium persulfate (APS, Wako Pure Chemical Industries. Ltd.) were used as received. Tetrahydrofuran (THF, commercial grade) was used as a carrier solvent for GPC. Deionized and distilled (DDI) water was used throughout the polymerization reaction and analysis.

Preparation of Seed Particles

The seed latices were prepared by the conventional emulsion polymerization. SDS and ammo-

nium persulfate (APS) were used as emulsifier and initiator, respectively. ST or MMA monomer was dispersed in SDS aqueous solution in a four-necked, 1000-mL flask. Nitrogen gas was gently bubbled through the dispersion for 1 h before the temperature was gradually raised to 343 K. APS solution (20 mL), after a thorough bubbling by nitrogen, was added in the reactor. The polymerization was carried out for 4 h at 343 K under a nitrogen atmosphere. The recipes of seed latex preparation and the properties of the seed latex are shown in Tables I and II.

To remove free SDS and undecomposed initiator as thoroughly as possible, the seed latex was filled in Visking membranes, dialyzed 2 days under the continuous flow of tap water, and then immersed in DDI water (replaced every day) for 5 days. After this treatment, the electroconductivity of the dialyzed latex became constant (about 12 $\mu\text{S}/\text{cm}$).

Thermally Initiated Seed Emulsion Polymerization

The thermally initiated seed emulsion polymerization was carried out in a four-necked, 500-mL flask immersed in a thermostat. The flask was equipped with a stirrer, condenser (nitrogen outlet), nitrogen inlet tube, and charge inlet for ingredients. A slow stream of nitrogen was introduced into the reaction mixture for 2 h after the weighed portion of monomer, seed latex, and DDI water with dissolved SDS were added into the flask. The stirrer was rotated at a rate of 350 rpm. Then the mixture was heated to 373 K in 30 min with a programmed heating device (Yamato Thermo-Mate BF 600, Yamato). A blanket of nitrogen atmosphere was maintained throughout the reaction period. In the runs accompanied with preswelling of the seed particles, the mixtures of monomer and SDS aqueous solution were treated by an homogenizer at 4000 rpm for 20 min, and the seed latices were swollen by monomer for 24 h under a nitrogen blanket before the seed emulsion polymerization started.

Table II Properties of Seed Polymer Particles

Run No.	Polymer Yield (g/l-Lx)	\bar{M}_w ($10^5/\text{g/mol}$)	\bar{M}_n ($10^5/\text{g/mol}$)	\bar{M}_w/\bar{M}_n (-)	dp (μm)	CV (%)
1901	300	25.1	8.03	2.51	0.12	12.7
1902	288	18.1	8.45	2.14	0.13	12.5

Table III Recipes of Seed Emulsion (Co)polymerization

Run No.	MMA (g)	ST (g)	SDS (g)	APS (g)	Seed Latex (g) (Solid Content)	Water (g)	Used Seed No.
2901/2902	/	25	0.1	/	83.3 [25]	391.6	1901
2903	10	15	0.1	/	83.3 [25]	391.6	1901
2904	15	10	0.1	/	83.3 [25]	391.6	1901
2906	25	/	0.1	/	86.7 [25]	388.2	1902
2907	15	10	0.1	/	86.7 [25]	388.2	1902
2908	/	12.5	0.1	/	83.3 [25]	404.1	1901
2909	/	50	0.1	/	83.3 [25]	366.4	1901
2910/2911	/	25	0.1	0.15	83.3 [25]	391.5	1901

Runs 1901 and 1902 are PMMA and PST seed, respectively. The reaction temperature is 373 K, the agitation rate is 350 rpm, and the reaction time is 18 h for run 2901–2909, and 3 h for runs 2910, and 2911. In run 2901 and run 2911, the mixture of styrene monomer and SDS aqueous solution is treated by homogenizer at 4000 rpm for 20 min, and the PMMA seed latex is swollen by styrene monomer for 24 h before the seed emulsion polymerization started.

Analyses

The polymer yield and the conversion of monomer were determined gravimetrically. Methanol was used to precipitate the polymer particles. The precipitated polymer was collected by a centrifuge, thoroughly washed with methanol two times, dried at 333 K in a drier, and weighed.

The average diameter of the particles was determined by direct measurement of 200 particles in a scanning electron microscope photograph (SEM, JSM-5310, JEOL).

The number- and weight-average molecular weights of polymer, \bar{M}_n and \bar{M}_w , were measured by gel permeation chromatography (GPC, HLC-8020, Tosoh) with the column system calibrated with standard PST. Commercial grade tetrahydrofuran was used as a carrier solvent.

The polymer particle morphology was observed by transmission electron microscopy (TEM, H-700H, Hitachi) with the samples stained with RuO_4 vapor.

RESULTS AND DISCUSSIONS

Effect of Monomer Composition in the Seed Particle

The thermally initiated seed emulsion polymerizations were carried out employing different seed particles, PMMA, and PST. The recipes are shown in Table III, and the analyzed properties are shown in Table IV.

In runs 2901 and 2911, preswollen polymer particles were employed. From SEM observation,

Table IV Main Properties of Polymer Latices Obtain from Seeded Emulsion (Co)polymerization

Run No.	Monomer Conversion (%)	\bar{M}_w (10^5 g/mol)	\bar{M}_n (10^5 g/mol)	\bar{M}_w/\bar{M}_n (–)	dp (μm)	CV (%)	ζ potential (mV)
2901	99.0	21.9	8.08	2.71	0.14	11.9	–32.6
2902	96.2	20.9	9.17	2.28	0.14	12.5	–39.5
2903	91.2	19.7	6.89	2.86	0.14	12.2	–33.3
2904	91.8	18.3	5.45	3.36	0.14	13.4	–31.5
2906	99.3	20.7	8.24	2.52	0.15	12.3	–29.9
2907	83.7	17.2	6.21	2.76	0.15	12.8	–33.5
2908	100	22.5	3.23	6.97	0.14	11.6	–30.2
2909	83.9	21.5	10.3	2.09	0.14	12.3	–37.1
2910	100	18.8	8.90	2.11	0.14	11.9	–69.7
2911	100	11.9	4.46	2.66	0.14	12.6	–79.92

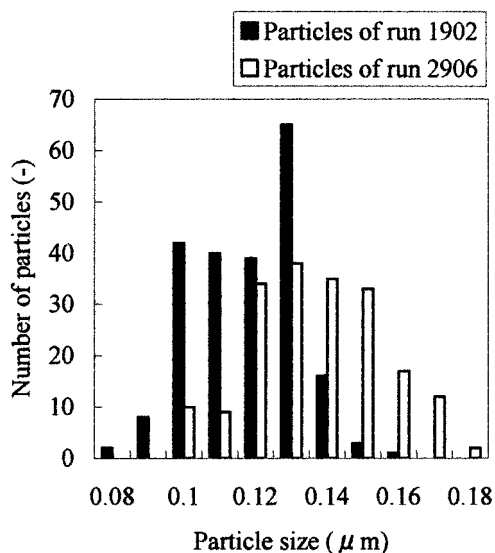


Figure 1 Particle size distribution. (run 1902: PST seed; run 2906: the final latex with MMA monomer).

no secondary nucleation occurred under the reaction conditions shown in Table III. The surface coverage of SDS is considered to be sparse. For example in run 2906, the amount of SDS required for the saturation adsorption on the surface of the seed particles (run 1902) is calculated to be 1.29 g by taking the adsorption area of SDS molecule on PST as 43 \AA^2 .²² From the recipe shown in Table III, the maximum amount of SDS possibly present in run 2906 is 0.36 g. It can be said that all the seed polymerizations were carried out with little free SDS in the aqueous phase. The effect of SDS on morphology development is not discussed in this work. From Table IV, it is clear that the polydispersity of polymer particles obtained by thermally initiated emulsion polymerization (above 30% of CV value)^{16,17} was improved by using the seed process, and the monodispersity of particles was the same as that of conventional seed emulsion polymerization. Figure 1 shows the particles size distribution of seed latex (run 1902) and the latex after seed emulsion polymerization (run 2906).

Runs 2902 and 2906 were carried out employing PMMA and PST seed latex, respectively, and the weight ratios of monomer to polymer (M/P) were fixed at 1. TEM photographs of polymer particles formed by runs 2902 and 2906 are shown in Figure 2(a) and (b), respectively. From Figure 2(a), three kinds of morphologies, hemispherical, sandwich-like, and inverted core-shell, were observed in the PMMA-seed emulsion poly-

merization of styrene. On the other hand, clear core-shell particle morphology was formed in the PST-seed emulsion polymerization of MMA [Fig. 2(b)]. In both cases, the PST-rich and PMMA-rich phase were normally separated clearly. Styrene and MMA monomer were common solvents to PST and PMMA, but at high polymer concentration the PST and PMMA phase started to separate.^{23,24} The viscosity of polymerization loci increased with the progress of polymerization, and consequently, the mobility of polymer molecules was restricted, and the phase separation was enhanced.

Matsumoto et al.²⁵ showed that, in the hydrophilic-hydrophobic polymer pair system, the

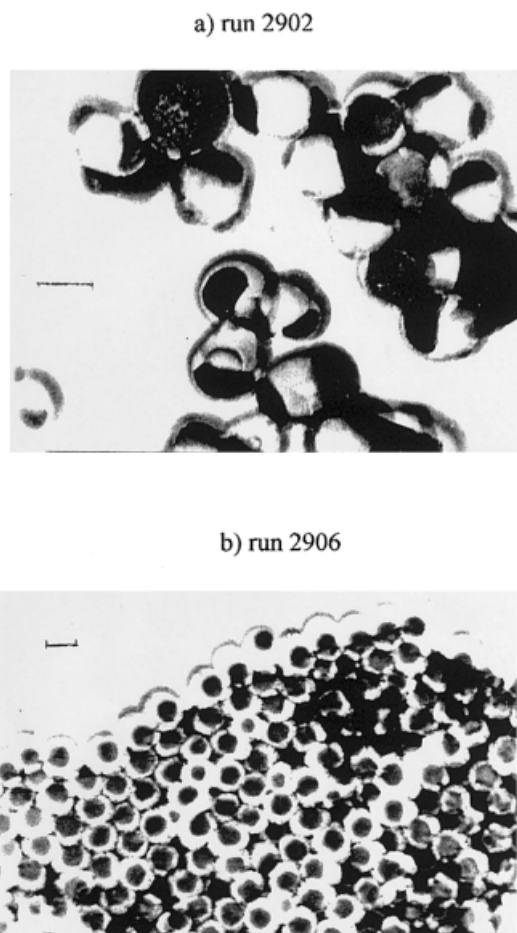


Figure 2 TEM photographs of polymer particles obtained from using different seed polymer particles. (a) PMMA is used as seed particles (run 2902); (b) PST is used as seed particles (run 2906), and the weight ratios of monomer to seed particles are 1. The polymer particles are stained with RuO_4 . The dark regions are polystyrene rich domains, and the lighter regions are PMMA rich domains. The scales are 100 nm.

morphology of particles depended on the hydrophilicity, stage ratio, molecular weight, viscosity, and polymerization methods. When hydrophobic monomers were polymerized with hydrophilic polymer seeds, it was shown that the hydrophobic domains were surrounded by hydrophilic ones. However, in the present system, the morphologies in which secondary polymers surrounded the seed polymer were dominant, although inverted core-shell morphology was formed [Fig. 2(a)]. It can be correlated to the initiation mechanism that may be dominant at the particle surface. In thermally initiated seed emulsion polymerization, because the monomers were used immediately after the distillation, the contribution from the hydroperoxide was regarded to be small. The high decomposition rate of hydroperoxide^{16,17} quickly reduced this contribution to zero. The Mayo mechanism,²⁶ tri-molecular initiation, is also unlikely to act as a major source of initiator radicals because monomers are absorbed in the polymer particles and present in a highly viscous environment. The generated radicals are likely to be deactivated before reacting with monomers and propagating. This leaves only one possible initiation—the complex formation between SDS and monomers proposed by Imoto-Ouchi¹³—and this was considered as the main source of radical generation. When two radicals are generated at the surface of particles, to start effective initiation, the generated radical pair should be separated by desorption of one radical into the aqueous phase.⁹ Moreover, at the particle surface, the radical re-entry to the particle from the aqueous phase can increase the local radical concentration. Due to this mechanism, the polymerization rate of seed polymerization was faster than that of the thermally initiated emulsion polymerization: the seed polymerization was almost completed in 8 h compared with about 80% monomer conversion of batch polymerization¹⁷ in 24 h under the same polymerization temperature.

In addition, the cause for the morphological difference between the two cases can be related to hydrophilicity. In the case using PST as the seed particle, as shown in Figure 2(b), clear core-shell morphology was formed due to the hydrophilicity of PMMA, despite the fact that the PST chains possessed a polar end group. In the case of using PMMA with polar end groups as the seed particles, PST was not able to dominate the surface because phase separation and migration of hydrophilic PMMA chains to the particle surface occurred simultaneously.

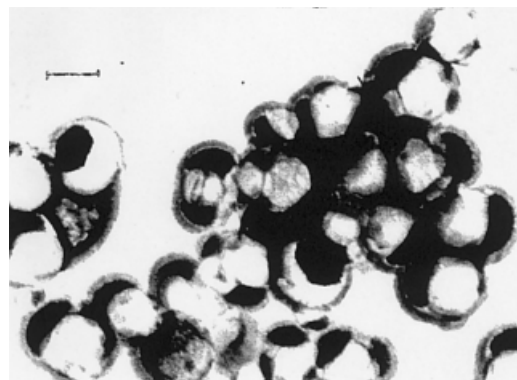


Figure 3 TEM photograph of polymer particles obtained from employing preswelling of seed particles. The mixture of styrene monomer and SDS aqueous solution is treated by homogenizer at 4000 rpm for 20 min, and the PMMA seed latex is swollen with styrene monomer for 24 h before the seed emulsion polymerization started. The weight ratio of monomer to seed particles is 1. The polymer particles are stained with RuO_4 . The dark regions are polystyrene rich domains, and the lighter regions are PMMA rich domains. The scale is 100 nm.

Effect of Preswelling of Polymer Particles

Matsumoto and his coworkers²⁵ claimed that the particle morphology was affected by the swelling state. Min and his coworkers²⁷ reported that the swelling state affected the formation of grafted copolymers and the long-term morphology change of P(butyl acrylate-*co*-ST) composite latex particles.

To investigate the effect of monomer swelling in polymer particles on particle morphology, run 2901 was carried out. The recipe was the same as for run 2902. A TEM photograph of the polymer particles obtained is shown in Figure 3. It is clear that the particle morphology in Figure 3 is same as that shown in Figure 2(a) (run 2902). Cho and Lee¹¹ found that the particle morphology and the rate of polymerization were not affected by the swelling time in their system, because the swelling rates of PMMA latices with styrene at room temperature was above 1 g/g per hour, and equilibrium swelling at polymerization temperature was attained during the nitrogen purge and heating period. In the present polymerization procedure, a slow stream of nitrogen was introduced into the reaction mixture for 2 h after the weighed portion of monomer was added to the reactor. The absence of a morphological difference may be due to the equilibrium swelling attained during the nitrogen purge and heating interval.

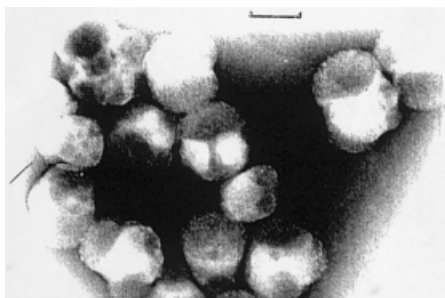


Figure 4 TEM photograph of polymer particles obtained by conventional seed emulsion polymerization. The polymer particles obtained from conventional seed emulsion polymerization using APS as an initiator are stained with RuO_4 . The weight ratio of monomer to seed particles is 1. The dark regions are polystyrene rich domains, and the lighter regions are PMMA rich domains. The scale is 100 nm.

Effect of Polymer Chain Ends

The anchoring effect of initiator-to-particle morphology has been suggested by many investigators.^{5,6,11} In the present system, no initiators were used in the seed polymerization stage. It should be kept in mind that the seed polymers possess anionic chain ends $-\text{SO}_4^-$ originating from the initiating radicals or the polar hydroxyl group formed by the hydrolysis of sulfate ion, while the secondary copolymers formed during the seed polymerization have none of those ends. Also, the monomer conversion, contrary to the batch runs, attained almost 100% regardless of the composition of monomers. Hence, it is expected to yield a different morphological form compared with the conventional initiator system. The reaction condition of run 2910 corresponds to that of run 2902, except that the initiator APS was used in the seed polymerization. Notice the ζ potential value shown in Table IV. It is clear that the absolute values of the ζ potential of polymer particles obtained from APS initiated seed emulsion polymerization were higher than those of thermally initiated seed emulsion polymerizations. A TEM photograph of polymer particles obtained from run 2910 is shown in Figure 4. Comparing Figure 4 with Figure 2(a), the same morphologies such as hemisphere-like and sandwich-like structures were obtained. Although the difference may not be clearly distinguishable, the boundary between the two domains was obscured in Figure 4, implying that the polystyrene chains with SO_4^- end group became slightly compatible with PMMA, because APS was used as the initi-

ator in seed particle preparation and seed polymerization.

This trend was clearer in the cases of runs 2901 and 2911, which employed sufficient preswelling of seed particles. Figure 5 shows a TEM photograph of run 2911 particles using APS as initiator. In this case, PST domains were randomly distributed in the particles, even in the particle core. PST gained some hydrophilicity comparable to PMMA by introducing initiator fragment SO_4^- to polymer chain ends, and consequently, the boundary between PST and PMMA became unclear. Moreover, comparing Figure 5 with Figure 3, the initiation at particle surface of thermally initiated seed emulsion polymerization were more evident.

Effect of Weight Ratio of the Secondary Monomer to Polymer (M/P)

In kinetically controlled morphologies, the key factor that determines the final particle morphology is the amount of second-stage monomer during the polymerization process. The thermally initiated PMMA-seed emulsion polymerization of styrene was carried out using different weight ratios of monomer to seed particle (M/P) : M/P weight ratios of runs 2908, 2902, and 2909 is 0.5/1, 1/1, and 2/1, respectively. TEM photographs



Figure 5 TEM photograph of polymer particles obtained by conventional seed emulsion polymerization, and employing preswelling of seed particles. The mixture of styrene monomer and SDS aqueous solution is treated by homogenizer at 4000 rpm for 20 min, and the PMMA seed latex is swollen by styrene monomer for 24 h before the seed emulsion polymerization. The weight ratio of monomer to seed particles is 1. The polymer particles obtained from conventional seed emulsion polymerization using APS as an initiator are stained with RuO_4 . The dark regions are polystyrene rich domains, and the lighter regions are PMMA rich domains. The scale is 100 nm.

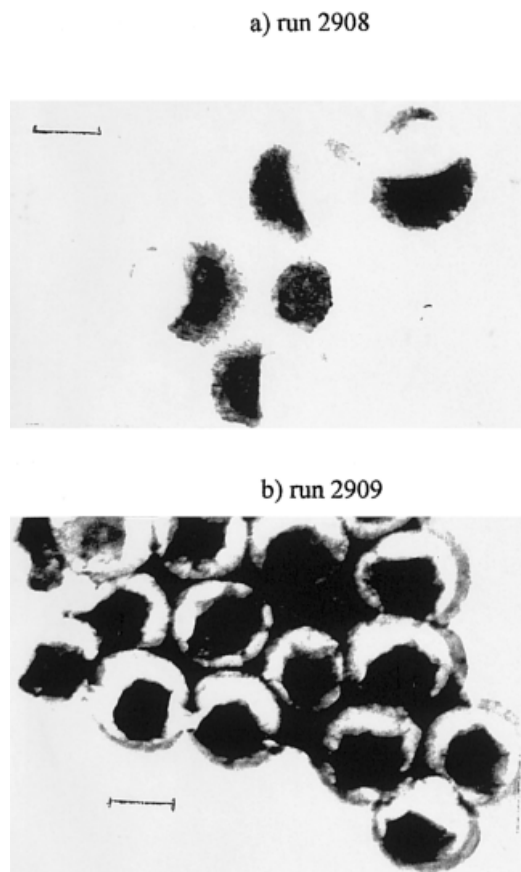


Figure 6 TEM photographs of polymer particles obtained from using different weight ratio of secondary monomer to seed polymer. In both cases, The PMMA is used as a seed particle, and the weight ratio of monomer to the seed particles is (a) 0.5/1, and (b) 2/1, respectively. The polymer particles are stained with RuO_4 . The dark regions are polystyrene rich domains, and the lighter regions are PMMA rich domains. The scales are 100 nm.

of final polymer particles obtained from 2908 and 2909 are shown in Figure 6(a), and (b), respectively. From Figure 6 and Figure 2(a) (run 2902), it can be seen that when the weight ratios of M/P increased from 0.5/1 to 1/1, and to 2/1, the particle morphologies changed from a hemisphere type (run 2908) to a hemisphere, sandwich, and inverted core-shell type (run 2902), and to an inverted core-shell type (run 2909). When the M/P weight ratio increased, the viscosity in the polymer particles reduced, and consequently, the mobility of polymer chains increased. The relatively hydrophilic polymer, PMMA with SO_4^- end groups migrated to the surface, and the hydrophobic polymer, PST, migrated to the core. In the case of run 2908 [Fig. 6(a)], the styrene monomer

polymerized at the surface, but was not able to migrate to the core because of the higher viscosity in the particles. On the other hand, in the case of run 2909 [Fig. 6(b)], the PST, which polymerized at the surface was able to migrate to the core due to the lower viscosity in the particles, and consequently, the inverted core-shell morphology was formed.

Effect of the Monomer Composition in the Seed Emulsion Copolymerization Stage

In our thermally initiated emulsion copolymerization, as shown in Table V, different morphologies were observed when the charged monomer composition of ST to MMA was varied. In our previous work,¹⁷ stalled (dead end) polymerizations were repeatedly observed when the monomer composition was selected at 50–60% of MMA. Monomer conversion leveled off at around 60%. On the other hand, 80% monomer conversion was achieved when the feed monomer composition was 20% MMA, rich in ST. The comparison of the particle morphologies between these two experiments, runs 901 and 908, is shown in Figure 7. From the size of these polymer particles (ca. 0.1 μm), there is no doubt that we observed well-grown particles: notice that the particle nucleation continued even at the final stage.^{16,17} Although the polymer particles of run 901 were stained in homogeneous tone [Fig. 7(a)], those of run 908 revealed a thin shell of MMA-rich domain surrounding the dark core as shown in Figure 7(b). For better understanding of the morphology development, the instantaneous and cumulative MMA composition in copolymer is plotted against the polymer yield, as shown in Figure 8(a). These are calculated from the modified Lewis-Mayo equation derived by considering the partition of MMA in the aqueous phase and oil phase (polymer particles and monomer droplets).¹⁷ The reactivity ratios are $\gamma_{\text{MMA}} = 0.46$ and $\gamma_{\text{ST}} = 0.523$. Although the solubility of ST in the aqueous phase is not considered in this

Table V Recipes of Thermally Initiated Emulsion Copolymerization

Run No.	ST (g)	MMA (g)	SDS (g)	Water (g)
901	25	25	3.5	446.5
908	40	10	3.5	446.5

Reaction temperature is 373 K, reaction time is 24 h, and the agitation rate is 350 rpm.

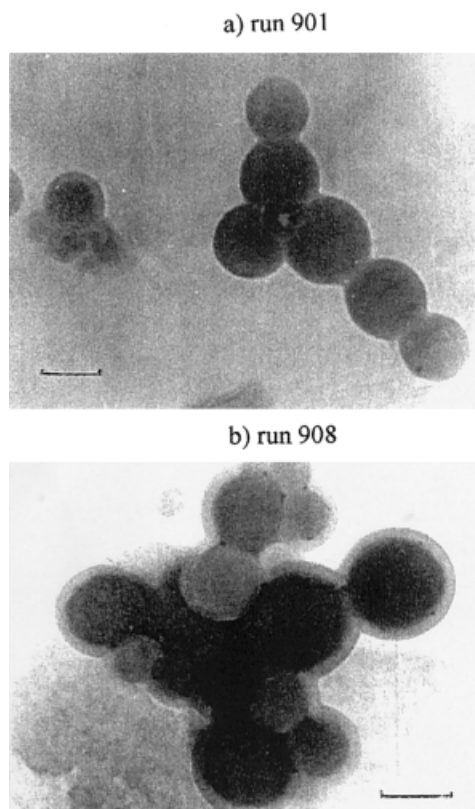


Figure 7 TEM photographs of polymer particles obtained from thermally initiated emulsion copolymerization. Thermally initiated emulsion copolymerization. The polymerizations are carried out at 373 K, for 24 h, and employing different monomer composition. The weight ratio of ST/MMA is (a) 5/5, (b) 8/2, respectively. The polymer particles are stained with RuO_4 . The dark regions are polystyrene rich domains, and the lighter regions are PMMA rich domains. The scales are 100 nm.

model, the calculated values agreed well with the observed MMA compositions.^{17,18}

Considering that run 901 stalled at 65 g/kg polymer yield, there is no distinct composition drift in the two copolymers. Actually, the copolymer of run 908 has a more homogeneous composition due to the gradual transfer of MMA partitioned in the aqueous phase to the polymer particles. Therefore, it is unrealistic to think that the PMMA-rich shell shown in Figure 7(b) was formed by the localization of more hydrophilic, PMMA-rich chains. Instead, it is more reasonable to assume, that in the final stage of polymerization, MMA partitioned in the aqueous phase preferentially polymerized in the aqueous phase or at the interface, and was eventually adsorbed on the surface of polymer particles. As already men-

tioned, Imoto and Ouchi proposed the initiation mechanism between the pendant $-\text{SO}_3^- \text{Na}^+$ [styrene sodiumsulphonate (NaSS) in copolymer chain] and MMA. The morphology in Figure 7(b) suggests that such a mechanism is indeed possible to take place between SLS and MMA (and probably ST also).

To investigate the effect of monomer composition in the seed emulsion copolymerization stage, runs 2903 and 2904 were carried out employing PMMA seeds (run 1901), and with monomer compositions, 4/6 and 6/4 of MMA/ST ratios, respectively. TEM photographs of runs 2903 and 2904 are shown in Figure 9(a) and (b), respectively. The profiles of cumulative and instantaneous composition of MMA for the seed polymerization runs are shown in Figure 8(b). In the case of run 2902, in which only ST was used as a monomer, hemispherical, sandwich-like, and inverted core-shell type morphologies were formed [Fig. 2(a)]. The same mixed-particle morphologies were observed when the charged monomer composition of MMA/ST was 4/6, as shown in Figure 9(a). Moreover, as the charged monomer composition of MMA/ST was 6/4 in favor of MMA, the inverted core-shell morphology became dominant, as shown in Figure 9(b). Considering that the seed polymer was hydrophilic MMA with the polar chain ends, the eventual inversion of the core and shell is likely. The above shift in morphology seems to reflect the cumulative composition of MMA, as shown in Figure 8(b). As the composition of MMA in entire polymer particles got higher, the transition to the inverted core-shell morphology was favored. Also, the drift of (instantaneous) composition of MMA in run 2904 is very

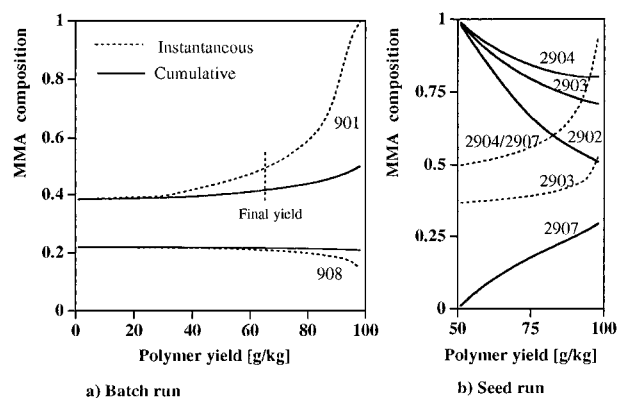


Figure 8 The instantaneous and cumulative MMA composition in copolymer plotted against the polymer yield.

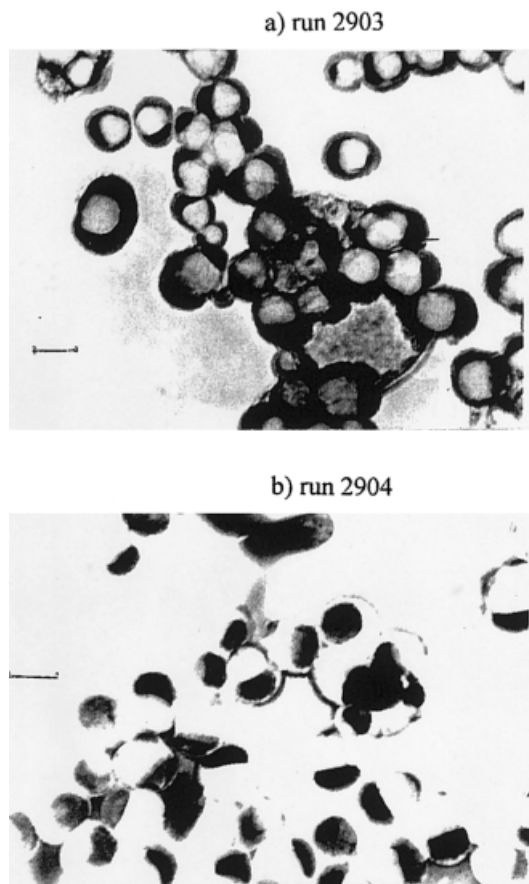


Figure 9 TEM photographs of polymer particles obtained from using PMMA seed particles, and varying the monomer composition. PMMA are used as seed particles, the weight ratios of monomer to seed particles are 1, and the charged monomer composition is (a) 6/4 (ST/MMA) (run 2903), (b) 4/6 (ST/MMA) (run 2904), respectively. The polymer particles are stained with RuO_4 . The dark regions are polystyrene rich domains, and the lighter regions are PMMA rich domains. The scales are 100 nm.

broad, indicating that the copolymers with more than 60% MMA started to form in the later stage of polymerization (from 83 g/kg polymer yield). These high MMA copolymers may be preferentially formed in the shell domain.¹⁰ On the other hand, in run 2903, the composition drift in the later stage is not as significant as for run 2904, and the resulting morphology remained similar to run 2902. The shadowy PMMA (and MMA-rich copolymer) domain compared to run 2902 may imply improved compatibility between the two domains because of the presence of the copolymer chains.

In the case employing PST seed particles for run 2907, a clear inverted core-shell morphology

was observed, as shown in Figure 10, even though the charged monomer composition for the seed polymerization was 6/4 in favor of the hydrophilic MMA. Figure 10 reveals a shadowy core, which implies a considerable composition of ST being present in the core. However, it is clear that the staining of the shell is darker. The contrast between the morphology of run 2906 (core-shell with 100% MMA monomer) and that shown in Figure 10 (inverted core-shell with 60% MMA comonomer) is quite instructive. Although the composition drift of run 2907 is identical with run 2904, and indeed almost 100% MMA copolymer can be formed towards the end of polymerization, it is not sufficient to form an MMA-rich shell as was present for run 2906. Again, the core was stained shadowy, implying improved compatibility between PST and the copolymers.

To conclude our series of morphology analysis, although the number of experiments was rather limited, the ranking of hydrophilicity (polarity) of polymers involved can be determined as follows: PMMA with ionic (polar) chain ends > PMMA with no ionic ends > PST with ionic ends > 60% MMA P(MMA-co-ST) with no polar ends > 40% MMA P(MMA-co-ST) with no polar ends > PST with no polar ends.

Apparently, no thin shell composed of rich MMA [Fig. 7(a)] was observed in these polymer particles formed by the seed polymerization. The principal differences are the presence of ionic

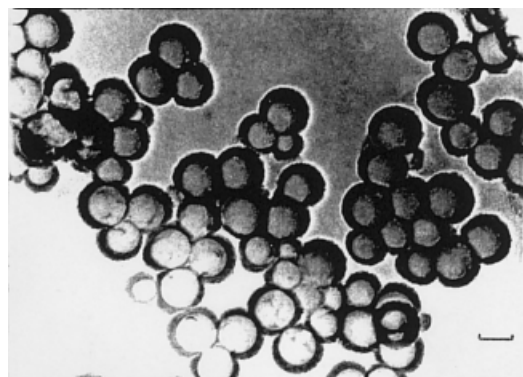


Figure 10 TEM photograph of polymer particles obtained from using PST seed particles, and employing 6/4 of MMA/ST monomer composition. PST is used as seed particles, the weight ratio of monomer to seed particles is 1, and the charged monomer composition is 4/6 (ST/MMA) (run 2907). The polymer particles are stained with RuO_4 . The dark regions are polystyrene rich domains, and the lighter regions are PMMA rich domains. The scale is 100 nm.

chain end groups ($-\text{SO}_4^-$) on the surface of seed particles, preswelling of comonomers in the seed particles, and the almost 100% monomer conversion attained in the seed polymerizations. Although our model¹⁷ is unable to distinguish the difference, there may be a slight difference of MMA partition in the aqueous phase between the batch and seed polymerization. A lesser amount of MMA may remain in the aqueous phase in the seed polymerization, while more MMA could remain in the batch polymerization because the polymerization always stalled at around 80% monomer conversion. We are still investigating how this difference in morphology development could possibly provide an insight to solve the initiation mechanism in thermally initiated emulsion polymerization.

The advantage of adopting thermally initiated (seed) emulsion polymerization for the study of morphology development is that one is able to form polymers with no polar chain ends and to control the hydrophilicity by the choice of monomer pair and compositions for the seed polymerization.

CONCLUSION

Poly(methyl methacrylate-*co*-styrene) composite latices were prepared by thermally initiated seed emulsion (co)polymerization of styrene (ST), methyl methacrylate (MMA), or ST and MMA employing PST or PMMA seed in the absence of conventional initiators. The seed polymer particles were prepared by using sodium dodecyl sulfate (SDS) as emulsifier, and ammonium persulfate (APS) as initiator. They were used for seed polymerization after exhaustive dialysis for 7 days. The size distribution of polymer particles obtained from the thermally initiated emulsion (co)polymerization improved, becoming narrower by employing the seed process. The development of particle morphology, observed by transmission electron microscopy (TEM), was investigated by varying seed particle component, the weight ratio of monomer to seed polymer, monomer composition, and employing preswelling of the seed particles. Hemispherical, sandwich-like, core-shell, and inverted core-shell particle morphologies were observed depending upon the polymerization conditions. The preswelling of seed particles did not affect to morphology of final particles because of the equilibrium swelling attained during the nitrogen purge and heating interval, which

lasted for 2 h. Other than the different initiation mechanism, the M/P ratio and the hydrophilicity of monomer were the main factors affecting the final particle morphology in the present system.

The particle morphology obtained from the thermal process was compared with that obtained from the conventional seed emulsion polymerization. The incorporation of initiator fragment SO_4^- to polymer chain ends allowed the PST to gain some hydrophilicity, and consequently the rank of hydrophilicity (polarity) between polymers emerged as follows: PMMA with ionic (polar) chain ends > PMMA with no ionic ends > PST with ionic ends > 60% MMA P(MMA-*co*-ST) with no polar ends > 40% MMA P(MMA-*co*-ST) with no polar ends > PST with no polar ends.

Finally, the advantage of adopting thermally initiated (seed) emulsion polymerization for the study of morphology development is that one is able to form polymers with no polar chain ends and to control the hydrophilicity by the choice of monomer pair and compositions for the seed polymerization.

REFERENCES

1. Smith, W. V.; Ewart, R. H. *J Chem Phys* 1948, 16, 592.
2. Grancio, M. R.; Williams, D. J. *J Polym Sci* 1970, A-18, 2617.
3. Grancio, M. R.; Williams, D. J. *J Polym Sci* 1970, A-18, 2733.
4. Keusch, P.; Prince, J.; Williams, D. J. *J Macromol Sci Chem* 1973, A7, 623.
5. Napper, D. H. *J Polym Sci* 1971, A-19, 2089.
6. Vanderhoff, J. W.; Van den Hul, H. J.; Tausk, R. J. M.; Overbeek, J. Th. G. In *Clean Surfaces: Their Preparation and Characterization for Interfacial Studies*; Goldfinger, G., Ed.; Marcel Dekker: New York, 1970, p. 15; Van den Hul, H. J.; Vanderhoff, J. W. *Br Polym J* 1970, 2, 121; *J Electroanal Chem Interfacial Electrochem* 1972, 37, 161.
7. Chern, C. S.; Poehlein, G. W. *J Polym Sci. Polym Chem* 1987, 25, 617.
8. Chern, C. S.; Poehlein, G. W. *J Polym Sci. Polym Chem* 1990, 28, 3073.
9. Russell, G. T.; Napper, D. H.; Gilbert, R. G. *Macromolecules* 1988, 21, 2141.
10. Shen, S.; El-Aasser, M. S.; Dimonie, V. L.; Vanderhoff, J. W.; Sudol, E. D. *J Polym Sci. Polym Chem* 1991, 29, 857.
11. Cho, I.; Lee, K.-W. *J Appl Polym Sci* 1985, 30, 1903.
12. Hawket, B. S.; Napper, D. H.; Gilbert, R. G. *J Chem Soc Trans Faraday Soc* 1980, I, 76, 1323.

13. Imoto, M.; Ouchi, T. *J Macromol Sci. Rev Macromol Chem Phys* 1983, C(22)2, 247.
14. Asahara, T.; Seno, M.; Shiraishi, S.; Arita, Y. *Bull Chem Soc Jpn* 1972, 45, 2862.
15. Matsumoto, T.; So, I.; Izatsu, A. *Kobunshi Kagaku* 1969, 26, 234.
16. Du, Y.-Z.; Akita, N.; Nagai, M.; Omi, S. *Recnt Res Dev Polym Sci* 1999, 3, 457.
17. Du, Y.-Z.; Ma, G.-H.; Nagai, M.; Omi, S. *J Appl Polym Sci*, in press.
18. Du, Y.-Z.; Ma, G.-H.; Nagai, M.; Omi, S. Presented in the International Conference on Free Radical Polymerization: Kinetics and Mechanism 3–8 June 2001, I1 Ciocco, Tuscany, Italy.
19. Sudduth, R D. *J Appl Polym Sci* 1993, 48, 37.
20. Mayer, M. J. J.; Meuldijk, J.; Thoenes, D. *Chem Eng Sci* 1994, 49, 4971.
21. Du, Y.-Z.; Ma, G.-H.; Nagai, M.; Omi, S. *J Appl Polym Sci*, accepted.
22. Gilbert, R. G. *Emulsion Polymerization, a Mechanistic Approach*; Academic Press: London, 1995, p. 330.
23. Kern, R. J. *J Polym Sci* 1956, 21, 19.
24. Molau, G. E. (a) *J Polym Sci. Part A* 1965, 3, 1267; (b) 1965, 3, 4235.
25. Matsumoto, T.; Okubo, M.; Shibao, S. *Kobunshi Ronbunshu* 1976, 33, 575.
26. Mayo, F. R. *J Am Chem Soc* 1958, 80, 2465.
27. Min, T. I.; Klein, A.; El-Aasser, M. S.; Vanderhoff, J. W. *J Polym Sci Polym Chem Ed* 1983, 21, 2845.